Journal of Power Sources 186 (2009) 29–36

Contents lists available at ScienceDirect

Journal of Power Sources

journal homepage: www.elsevier.com/locate/jpowsour

Characteristics and performance of lanthanum gallate electrolyte-supported SOFC under ethanol steam and hydrogen

Bo Huang[a,*], Xin-Jian Zhu[a], Wan-Qi Hu[b], Qing-Chun Yu[a], Heng-Yong Tu[a]

[a] Institute of Fuel Cell, Shanghai Jiaotong University, 800 Dongchuan Road, Shanghai 200240, PR China
[b] Institute of Process Engineering, Chinese Academy of Sciences, PR China

ARTICLE INFO

Article history:
Received 23 July 2008
Received in revised form 5 September 2008
Accepted 8 September 2008
Available online 27 September 2008

Keywords:
Anode
Carbon deposition
Electrochemical impedance spectroscopy
LSGMC
Solid oxide fuel cell (SOFC)

ABSTRACT

This study is focused on the electrochemical performance of perovskite-type materials based on doped $LaGaO_3$. $La_{0.8}Sr_{0.2}Ga_{0.8}Mg_{0.2}O_{3-\delta}$ (LSGM) and $La_{0.8}Sr_{0.2}Ga_{0.8}Mg_{0.115}Co_{0.085}O_{3-\delta}$ (LSGMC) were used as electrolytes and $(Pr_{0.7}Ca_{0.3})_{0.9}MnO_3$ (PCM) and $La_{0.75}Sr_{0.25}Cr_{0.5}Mn_{0.5}O_{3-\delta}$ (LSCM) as cathode and anode material, respectively. LSGM and LSGMC electrolytes were prepared by tape casting with a thickness of about 600 μm. The performance of LSCM/LSGMC/PCM was slightly superior to that obtained on LSCM/LSGM/PCM at different temperatures in both humidified hydrogen and ethanol steam atmospheres, good values of power output in LSCM/LSGMC/PCM were 182 and 169 mW cm^{-2} using humidified hydrogen and ethanol steam as fuel, respectively, and oxygen as oxidant at 850 °C. Cell stability tests indicate no significant degradation in performance after 60 h of cell testing when LSCM anode was exposed to ethanol steam at 750 °C. Almost no carbon deposits were detected after testing in ethanol steam at 750 °C for >60 h on the LSCM anodes, suggesting that carbon deposition was limited during cell operation.

1. Introduction

Solid oxide fuel cell (SOFC) is an all solid device that converts the chemical energy of fuel gas such as hydrogen and natural gas to electricity through electrochemical processes. SOFC can provide high total efficiency when it is used in a cogeneration system and promise clean power sources with little production of NO_x and SO_x. Generally, it must be operated at high temperatures up to 1000 °C because the Y_2O_3 stabilized ZrO_2 (YSZ) is used as the conventional electrolyte material and has a low ionic conductivity at operating temperatures lower than 800 °C. Such high temperatures present significant problems for materials selection and durability, especially for smaller scale applications. Therefore, it is desired to develop SOFC operating at intermediate temperatures. To reduce the operation temperature, two approaches are under active considerations as follows: one is the reduction of the thickness of the YSZ electrolyte as thin as a few tens of micrometers [1], and another is the application of alternative electrolyte materials such as La(Sr)Ga(Mg)$O_{3-\delta}$ (LSGM) [2–4], which has a higher ionic conductivity than YSZ. In addition, SOFCs require hydrogen as the fuel, but viable near-term applications will need to use the more readily available hydrocarbons, such as methane. Therefore, it is important for fuel cell technology to achieve efficient electrode operation with different hydrocarbon fuels [5–10], although such fuels are more demanding than pure hydrogen.

However, the best anode materials to date – Ni-YSZ (yttria-stabilized zirconia) cermets [11] – suffer some drawbacks related to low tolerance to sulphur [12], volume instability on redox cycling and carbon deposition when using hydrocarbon fuels [13] since Ni is a good catalyst for hydrocarbon cracking reaction (though device modifications and lower temperature operation can avoid this [14,15]). Deposited carbon covers the active sites of the anode, resulting in rapid, irreversible cell deactivation [16–20]. Replacing Ni/YSZ cermet anodes by Ni-free oxide such as ceria, titanate and lanthanum chromite-based oxides has attracted a great attention recently.

The preparation and characterization of a new electrolyte material has been reported in the literature [21] based on LSGM with the addition of Co^{2+} in the B site of the perovskite structure, i.e., $La_{0.9}Sr_{0.1}Ga_{0.8}Mg_{0.115}Co_{0.085}O_{3-\delta}$ (LSGMC). Ishihara et al. [22] reported that the cobalt doping is effective for enhancing the oxide ion conductivity at low temperature compared to LSGM. Doped $LaCrO_3$-based materials have been extensively investigated as interconnect material in SOFC [23]. $LaCrO_3$-based oxide such as $(LaSr)CrO_3$ has shown very low activity towards carbon deposition [24]. Catalytic activity of $LaCrO_3$ for methane oxidation can also be substantially enhanced by partial substitution at A- and B-sites. Sfeir et al. [25,26] studied the thermodynamic stability and the catalytic activity of $(La,A)(Cr,B)O_3$ system (A = Ca, Sr and B = Mg, Mn, Fe, Co, Ni) as alternative anode materials under simulated SOFC

* Corresponding author. Tel.: +86 21 34206249; fax: +86 21 34206249.
E-mail address: huangbo2k@hotmail.com (B. Huang).

0378-7753/$ – see front matter © 2008 Elsevier B.V. All rights reserved.
doi:10.1016/j.jpowsour.2008.09.068

operation conditions. Thermodynamically, Sr and Mn substitution maintains the stability of the perovskite while other substitutes destabilize the system. Recently, Tao and Irvine [27,28] reported promising results of $La_{0.75}Sr_{0.25}Cr_{0.5}Mn_{0.5}O_3$ (LSCM) as anode for SOFC. LSCM is a p-type conductor with conductivity of ~38 S cm^{-1} in air and 1.5 S cm^{-1} in 5%H_2 at 900 °C. The electrode polarization resistance for the oxidation reactions in wet CH_4 and H_2 at 900 °C was 0.85 Ω cm^2 and 0.26 Ω cm^2, respectively. The performances are considered to be compatible to the Ni/YSZ cermet anodes.

Given the promising properties of Co-doped LSGM (LSGMC) electrolytes for the development of reduced-temperature SOFCs, in this work we continued our previous work on solid-state synthesis of dense LSGM electrolyte matrix [29] and present the electrochemical characterization of LSGMC electrolytes prepared by solid-state reaction method. LSGM and LSGMC were tested as electrolyte using $(Pr_{0.7}Ca_{0.3})_{0.9}MnO_3$ (PCM) and $La_{0.75}Sr_{0.25}Cr_{0.5}Mn_{0.5}O_{3-\delta}$ (LSCM) as cathode and anode, respectively. The fabrication and performance of electrolyte-supported system LSCM/LSGM/PCM and LSCM/LSGMC/PCM were investigated to assess their feasibility as alternative anode material for ethanol oxidation reactions for SOFC.

2. Experimental

2.1. Synthesis of electrode and electrolyte

The composition of LSCM anode was chosen as $La_{0.75}Sr_{0.25}Cr_{0.5}Mn_{0.5}O_{3-\delta}$ (LSCM) [27,28]. $La_{0.75}Sr_{0.25}Cr_{0.5}Mn_{0.5}O_{3-\delta}$ anode material was prepared using a combustion synthesis technique based on stoichiometric amounts of lanthanum nitrate ($La(NO_3)_3{\cdot}6H_2O$), strontium nitrate ($Sr(NO_3)_2$), chromium nitrate ($Cr(NO_3)_3{\cdot}9H_2O$) and manganese nitrate ($Mn(NO_3)_2$) and citric acid ($C_6H_8O_7{\cdot}H_2O$). Details of the preparation method can be found elsewhere [29]. The final sintering was achieved at 1200 °C for 5 h in air.

$La_{0.8}Sr_{0.2}Ga_{0.8}Mg_{0.2}O_{3-\delta}$ (LSGM) and $La_{0.8}Sr_{0.2}Ga_{0.8}Mg_{0.115}Co_{0.085}O_{3-\delta}$ (LSGMC) used as the electrolytes were prepared from stoichiometric amounts of La_2O_3 (>99.99% purity), $SrCO_3$ (>99.9% purity), Ga_2O_3 (>99.99% purity), MgO (>99.9% purity) and CoO (>99.9% purity) by traditional solid-state reaction method. Before weighing, La_2O_3 was heat-treated at 1000 °C for over 3 h in order to achieve decarbonation and dehydration. The powders were intimately mixed in an agate mortar with the aid of absolute alcohol for 24 h and then calcined at 950 °C for 10 h. The calcined powders were ground using agate mortar and pestle and ball-milled in absolute alcohol for another 24 h. The resulting fine powders were dried and uniaxially pressed into dense pellet (99% of theoretical density) and then sintered at 1500 °C for 6 h in air.

2.2. Preparation of LSGM (LSGMC) electrolyte matrix

The procedure for obtaining LSGM (LSGMC) electrolyte matrix by tape casting comprised the preparation of a slurry containing LSGM or LSGMC powder, azeotropic mixture of butanone and ethyl alcohol absolute as solvent; triethanolamine as a kind of zwitterionic dispersant to reduce the interfacial tension between the surface of the particle and the liquid; polyethylene glycol (PEG 200) as plasticizer to increase the flexibility of the tapes; and poly-vinyl-butyl (PVB) as binder to provide their strength after the evaporation of the solvent. The PVB binder was supplied as a free flowing fine-grained powder and the PEG plasticizer was obtained in a liquid form. All the organic additives were supplied by Shanghai Chem. Ltd., China. Intermediate ball-milling steps are used for the preparation of the tapes. After the mixing and the homogenization of the slurry were completed, the slurry was degassed using a vacuum pump (pressure: 200 mbar absolute) and cast on a casting surface of polyethylene film by a "doctor-blade" method. The cast tapes were allowed to dry at room temperature for 48 h. After the solvent in the tapes was completely evaporated, the LSGM or LSGMC green tapes were obtained. They were then sintered in air at 1500 °C for 6 h. Thus a disk-shaped electrolyte substrate, having a diameter of about 3.0 cm, a thickness of about 600 μm, was then produced.

2.3. Materials characterization

X-ray diffraction (XRD) patterns were collected with a Philips X'Pert Pro diffractometer equipped with a primary monochromator (Cu Kα radiation) and a Philips X'Celerator detector for the structural characterization of the specimens. The scans were performed in the 2θ range 20–90° at the scanning speed of 4° min^{-1}. Further XRD studies were also carried out to investigate the chemical compatibility of LSGM or LSGMC with LSCM and PCM materials. Powder mixtures of LSGM(LSGMC) with LSCM and LSGM (LSGMC) with PCM, in a 1:1 (wt.%) ratio, were ground in an agate mortar and fired at several temperatures for 10 h. Images of the interface layer LSGM (LSGMC)/LSCM before and after SOFC single cell operation were analyzed using Field emission scanning electron microscope (FE-SEM, PHILIPS 515, Holland) equipped

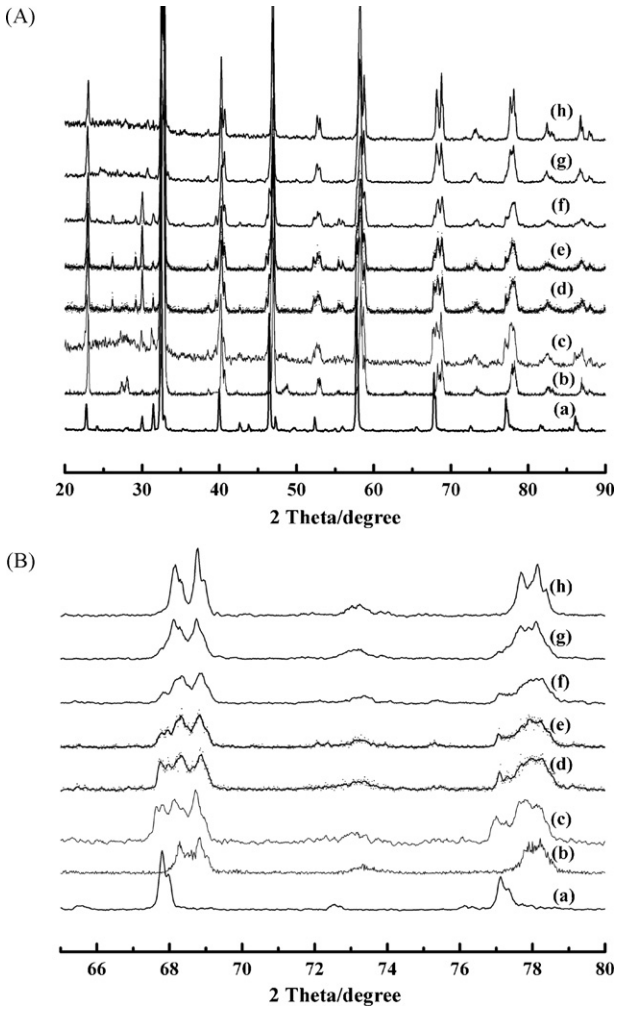

Fig. 1. XRD patterns of LSGM (a), LSCM (b), and LSGM + LSCM at the following temperatures: room temperature (c), 1000 °C (d), 1100 °C (e), 1200 °C (f), 1300 °C (g), 1400 °C (h) (A) and magnification in the 2θ range 65–80° (B).

with an X-ray analyzer for energy-dispersive X-ray spectroscopy (EDS).

2.4. Characterization of single cell performance

Single cell tests were carried out on a three-electrode arrangement using 20 mm diameter LSGM (LSGMC) pellets (600 μm thick) as electrolyte, PCM as cathode material, and LSCM as anode material. PCM was painted onto the electrolyte LSGM (LSGMC) (surface of π (0.7 cm)^2 = 1.5386 cm^2) and fired at 1200 °C for 3 h. The anode was prepared by coating a layer of LSCM slurry, using PVB as binder, onto the other side of electrolyte by screen-printing method and then firing at 1200 °C for 3 h in air. Experimental techniques, apparatus and the electrochemical cell assembly for SOFC tests have been described previously [29]. A Pt mesh and lead wire were attached to the surface of the cathode using a Pt ink, followed by sintered at 950 °C for 0.5 h. On the anode side, a Au mesh and lead wire were used as the current collector and were attached using a Au ink applied to the edges of the Au mesh, followed by sintering at 850 °C for 0.5 h. The anode side of the structure was then attached to an alumina tube using Au ink and the edges were sealed using a ceramic adhesive. All the anodes were evaluated with the same testing procedure. Hydrogen or gasified ethanol–water mixture (with volume ratio 2:1) were used as fuel and oxygen was used as oxidant. The fuel and oxidant flow rate were all controlled at 25 mL min^{-1}, and the liquid fuel was vaporized by water bath (70 °C) and then brought into the anode surface by nitrogen. The current–voltage curves and electrochemical impedance spectroscopy (EIS) were obtained using an Electrochemical Workstation IM6e (Zahner, GmbH, Germany). These measurements were started after stabilized under a constant discharge voltage of 0.7 V for 4 h in order to obtain a sufficiently stabilized system necessary for a cell testing experiment. Then the current was switched off and the impedance spectra of the electrochemical cell were recorded under open circuit from time to time with amplitude of 20 mV over the frequency range 0.02 Hz to 100 kHz. The measurement was carried out in the temperature range of 700–850 °C in steps of 50 °C. The ohmic resistance of the electrolyte, the cathode and the anode (RΩ)was estimated from the high frequency intercept of the impedance curves and the overall electrode polarization (interface) resistance (R_E) was directly measured from the differences between the low and high frequency intercepts on the impedance curves.

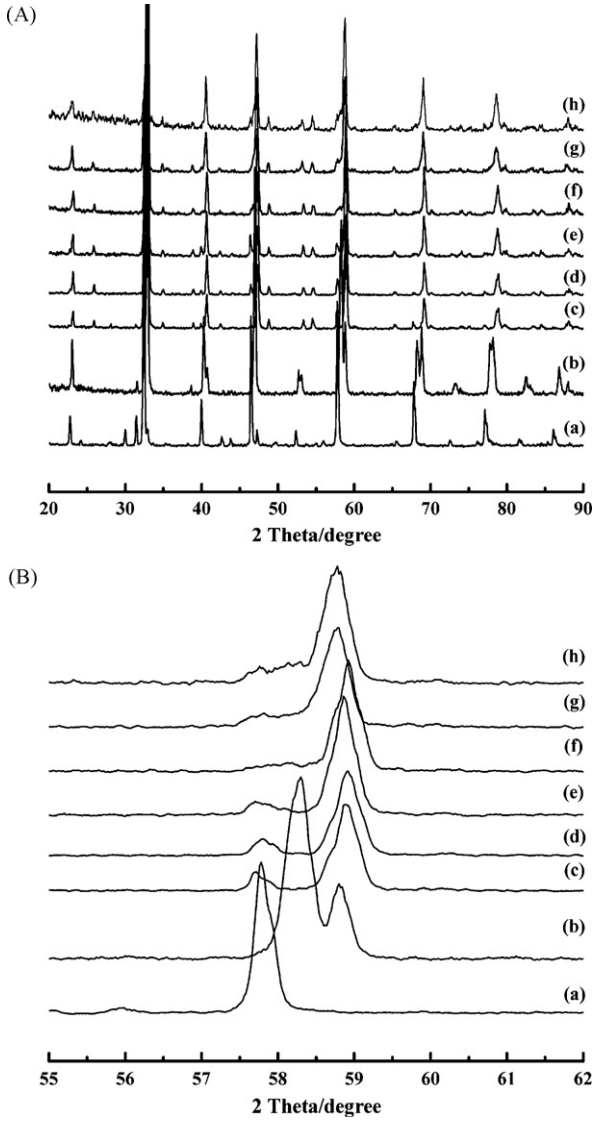

Fig. 2. XRD patterns of LSGM (a), PCM (b), and LSGM + PCM at the following temperatures: room temperature (c), 1100 °C (d), 1200 °C (e), 1250 °C (f), 1300 °C (g), 1400 °C (h) (A) and magnification in the 2θ range 65–80° (B).

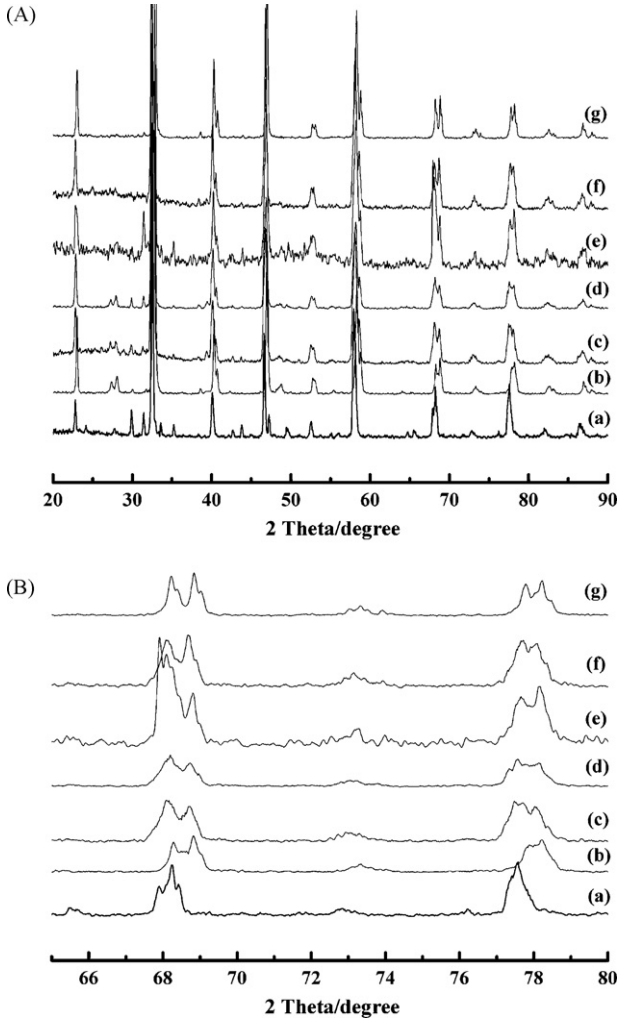

Fig. 3. XRD patterns of LSGMC (a), LSCM (b), and LSGMC + LSCM at the following temperatures: room temperature (c), 1100 °C (d), 1200 °C (e), 1300 °C (f), 1400 °C (g) (A) and magnification in the 2θ range 65–80° (B).

3. Results and discussion

3.1. Chemical compatibility study

The XRD patterns of the binary-mixed-systems LSGM/LSCM, LSGM/PCM and LSGMC/LSCM, LSGMC/PCM at different temperature are shown in Figs. 1–4. No additional diffraction peaks were found after firing mixtures of LSGM/LSCM and LSGM/PCM in the air for 10 h, between room temperature and 1200 °C indicating a good chemical compatibility at intermediate temperature (≤800 °C). Nevertheless, certain reactivity could be observed between LSGM and LSCM at 1300 °C, between LSGM and PCM above 1250 °C, between LSGMC and LSCM at 1200 °C and between LSGMC and PCM above 1200 °C. No reaction was observed for the LSGM/LSCM system at 1000–1200 °C. Du and Sammes [30] reported that no interactions were detected from XRD data in their experiments of fabrication of bilayer samples of LSGM and LSCM at 1500 °C for 2 h. However, they found severe reactions in samples after 6 h and over at 1500 °C, forming low conductive phases. They used energy-dispersive spectrometry (EDS) analysis to find reaction-diffusion zones in the range 50–150 μm. Nevertheless, they indicate from their overall results that LSCM is a thermomechanically and chemically compatible anode material with LSGM electrolyte at the fuel cell operating temperatures and fuel cell fabrication conditions (at 1500 °C for 2 h). In this work, LSCM material had been applied to the electrolyte LSGM at 1200 °C for 3 h, and LSGM and LSCM did not show apparently remarkable signs of reaction in fired compacted powder. These results indicate that LSCM is a thermomechanically and chemically compatible anode material with LSGM electrolyte at the fuel cell operating temperatures and fuel cell fabrication conditions (at 1200 °C for 3 h). However, the XRD pattern of the mixture LSGM/LSCM at 1300 °C for 10 h, Fig. 1(g), showed a reaction which becomes stronger at 1400 °C, Fig. 1(h). The XRD pattern of the mixture LSGMC/LSCM at 1200 °C for 10 h, Fig. 3(e), did not show apparently remarkable signs of reaction in fired compacted powder, indicating that LSCM is also a thermomechanically and chemically compatible anode material with LSGMC electrolyte at the fuel cell operating temperatures and fuel cell fabrication conditions (at 1200 °C for 3 h). The interaction between LSGMC/LSCM has not been studied further and more studies are necessary. In the PCM/LSGM(LSGMC) case, the PCM cathode material fired at 1200 °C onto LSGM(LSGMC) did not show obvious signs of reaction.

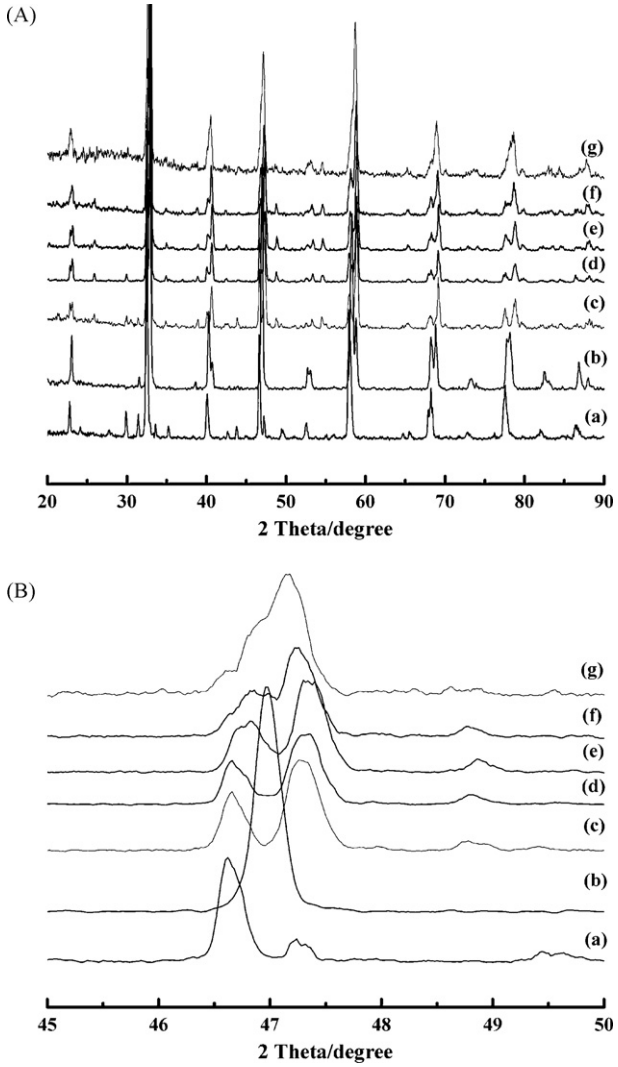

Fig. 4. XRD patterns of LSGMC (a), PCM (b), and LSGMC + PCM at the following temperatures: room temperature (c), 1100 °C (d), 1200 °C (e), 1250 °C (f), 1300 °C (g) (A) and magnification in the 2θ range 45–50° (B).

3.2. Fuel cell tests

3.2.1. Current–voltage measurements

Figs. 5 and 6 show typical voltage and power density *vs.* current density for a SOFC with the electrolyte-supported system

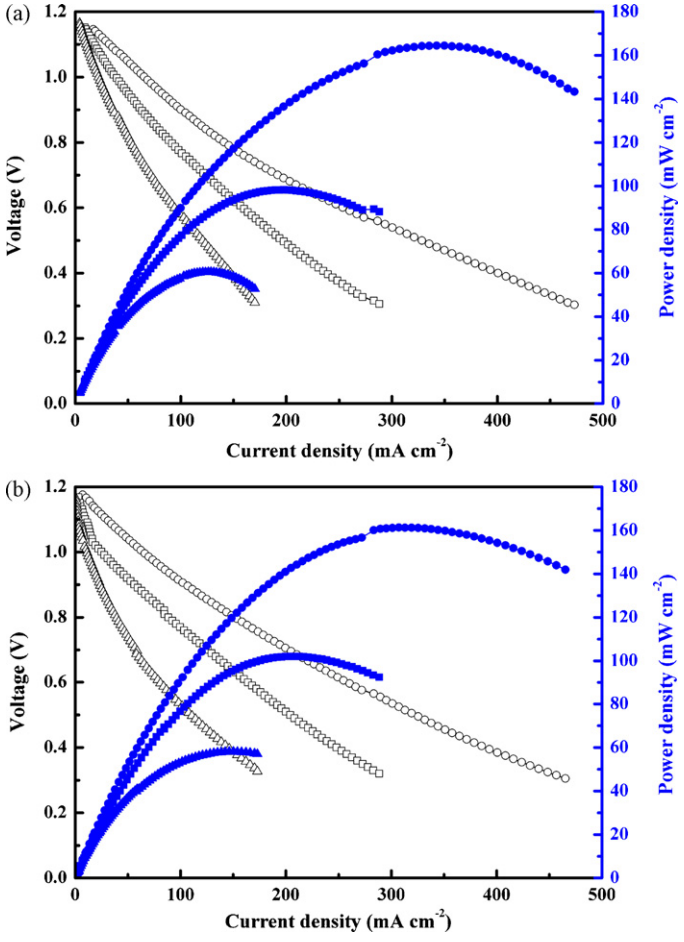

Fig. 5. Voltage and power density *vs.* current density for a SOFC with the electrolyte-supported system LSCM/LSGM/PCM at different temperature using humidified hydrogen (a) or ethanol steam (b) as fuel and oxygen as oxidant: (○,●)850 °C; (□,■) 800 °C; (△,▲)750 °C.

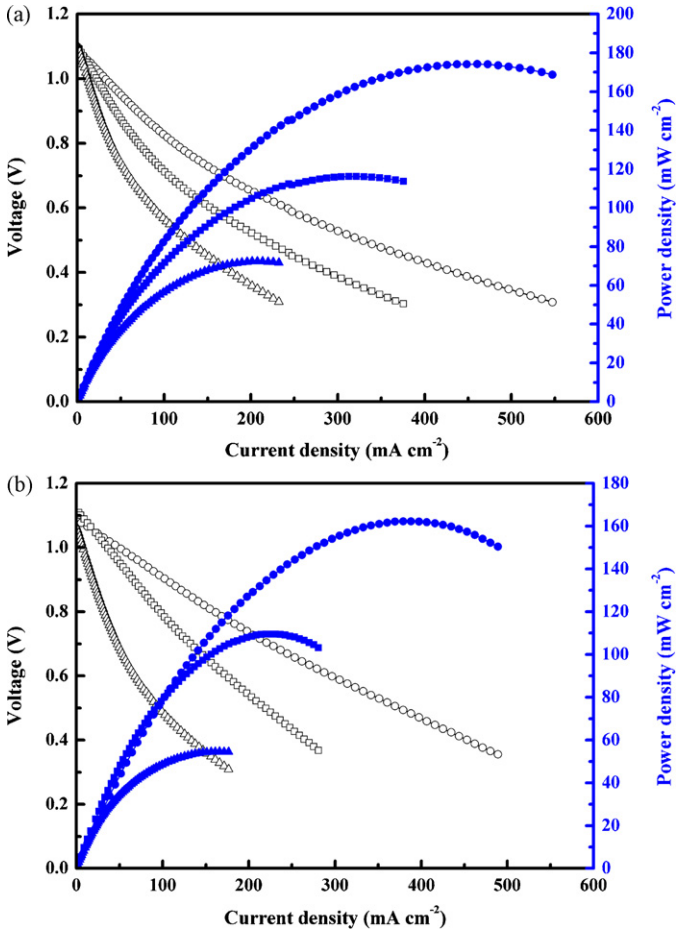

Fig. 6. Voltage and power density *vs.* current density for a SOFC with the electrolyte-supported system LSCM/LSGMC/PCM at different temperature using humidified hydrogen (a) or ethanol steam (b) as fuel and oxygen as oxidant: (○,●)850 °C; (□,■) 800 °C; (△,▲)750 °C.

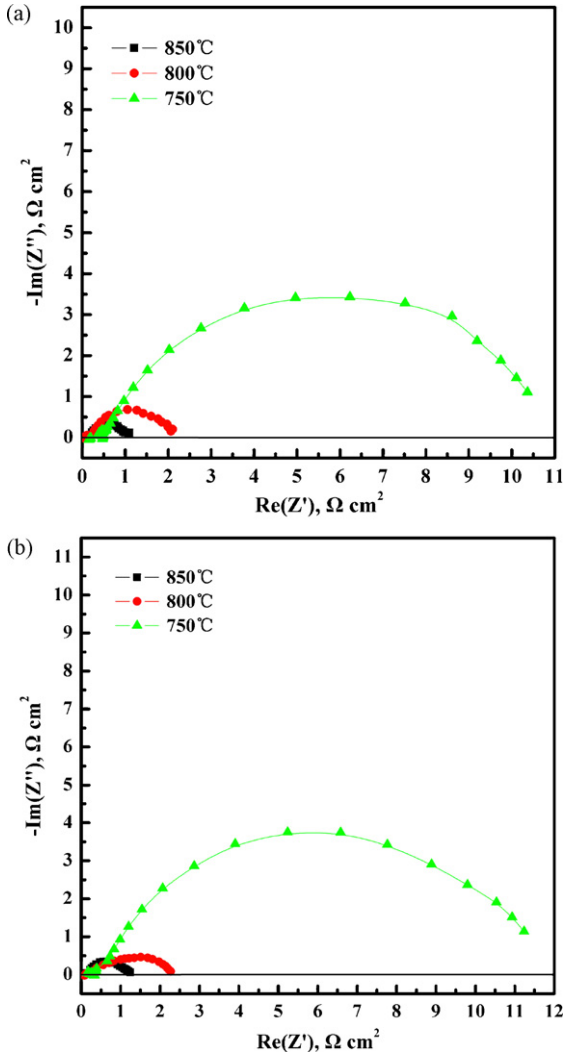

Fig. 7. Electrochemical impedance spectra for a SOFC with the electrolyte-supported system LSCM/LSGM/PCM at different temperature using humidified hydrogen (a) or ethanol steam (b) as fuel and oxygen as oxidant under open circuit.

LSCM/LSGM(LSGMC)/PCM while running on humidified hydrogen (a) and ethanol steam (b) at 850 °C, 800 °C and 750 °C, respectively. We could see that the open circuit voltages (OCV) of the cell LSCM/LSGM/PCM for H_2 and C_2H_5OH steam were respectively 1.146–1.165 V and 1.164–1.176VV in the temperature range, whereas the corresponding values were 1.086–1.108 V and 1.106–1.125 V for the cell LSCM/LSGMC/PCM. It revealed the electrolyte was dense enough that resulted in higher values of OCV. The performance of the cell LSCM/LSGM/PCM while operating on humidified hydrogen was modest with a maximum power density of 165 mW cm^{-2}, 99 mW cm^{-2} and 62 mW cm^{-2} at 850 °C, 800 °C and 750 °C, respectively, and whereas the corresponding values were 182 mW cm^{-2}, 125 mW cm^{-2} and 80 mW cm^{-2} for the cell LSCM/LSGMC/PCM. The highest power density of the cell LSCM/LSGM/PCM while operating on ethanol steam was 160 mW cm^{-2}, 101 mW cm^{-2} and 58 mW cm^{-2} at 850 °C, 800 °C and 750 °C, respectively. The counterpart of the cell LSCM/LSGMC/PCM while operating on ethanol steam was 169 mW cm^{-2}, 120 mW cm^{-2} and 68 mW cm^{-2} at 850 °C, 800 °C and 750 °C, respectively. The data show that the performance of the cell LSCM/LSGMC/PCM is slightly superior to that of the cell LSCM/LSGM/PCM. Taking into consideration the thickness of the electrolyte (600 μm) and the LSCM anode (65 μm), we have obtained feasible performance about the electrolyte-supported system LSCM/LSGM(LSGMC)/PCM while running on humidified hydrogen and ethanol steam at different temperature. Next work is to decrease the thickness of the electrolyte and the LSCM anode in order to improve the cell performance.

3.2.2. *Electrochemical impedance spectroscopy (EIS) study*

Figs. 7 and 8 show a comparison of typical EIS results, from cell with the electrolyte-supported system LSCM/LSGM(LSGMC)/PCM while running on humidified hydrogen (a) and ethanol steam (b) under open circuit at different temperature, respectively, associated with the *V–I* curves in Figs. 5 and 6. As could be expected through examination of Figs. 7 and 8, the cells exhibit less total impedance ($R\Omega + R_E$) in humidified hydrogen than that in ethanol steam at different temperature, and the LSCM/LSGMC/PCM cell exhibits less total impedance than that obtained on the LSCM/LSGM/PCM cell, which are in good agreement with the results shown in Figs. 5 and 6.

As to the microstructure, Fig. 9 shows the FE-SEM micrograph of the LSCM thick film (65 μm) sintered at 1200 °C for 3 h. The microstructure obtained is very promising, a highly porous structure made of sintered perovskite-structure particles. Fig. 10 shows the FE-SEM micrograph of the interface LSGM/LSCM (a) and LSGMC/LSCM (b) after fuel cell test in ethanol steam at 750 °C for 60 h, respectively. In general, the distribution of the grains in the

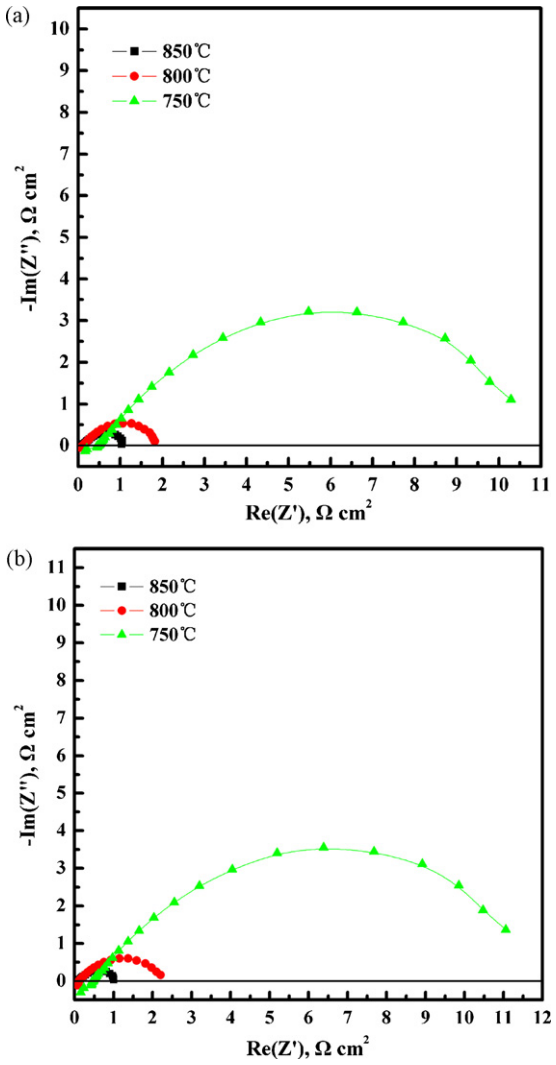

Fig. 8. Electrochemical impedance spectra for a SOFC with the electrolyte-supported system LSCM/LSGMC/PCM at different temperature using humidified hydrogen (a) or ethanol steam (b) as fuel and oxygen as oxidant under open circuit.

anode material is fairly homogeneous with an average grain size of 2 μm. Dense microstructures were observed also for LSGM and LSGMC pellets sintered in air, thus confirming that all samples exhibited a high density and a negligible amount of residual porosity. Moreover, the loss of adherence and partial grain agglomeration of LSCM material after fuel cell test shown in Fig. 10, is possibly other reasons for the lower electrochemical performance respect LSCM material-based systems. Microstructure and adherence of the PCM cathode also seem good (Fig. 11(a) and (b)). Therefore, in order to achieve comparable performances of the electrolyte-supported cell LSCM/LSGM(LSGMC)/PCM at 750 °C, further work will be done to reduce the thickness of LSCM anode film and electrolyte layer and improve the adherence between the anode and the electrolyte.

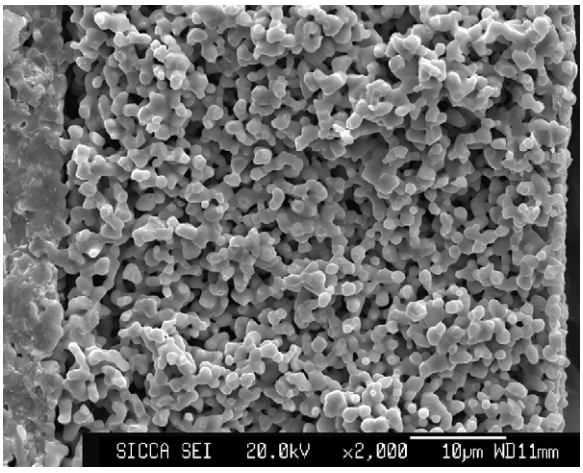

Fig. 9. FE-SEM micrograph of the LSCM thick film sintered at 1200 °C for 3 h.

3.3. Cell stability tests

The stabilization and degradation of the electrolyte-supported cell LSCM/LSGM/PCM and LSCM/LSGMC/PCM were also investigated in ethanol steam at 750 °C during the measurements. We recorded the curve of power density as a function of time for the cell operating on ethanol steam at 750 °C, shown in Fig. 12. We can find that the performance of the cell almost kept constant with a little augment of power density with time in the period of 60 h. In one case, the cell was operated for >60 h in ethanol steam at 750 °C, before the test was stopped with the cell still running well. Almost no carbon deposits were detected after testing in ethanol steam at 750 °C for >60 h on the LSCM anodes under conditions in the present study, suggesting that carbon deposition was limited during cell operation. Thus the cracking of ethanol is not likely the main reaction path on the LSCM anodes. Tao et al. investigated the catalytic activity of LSCM for methane oxidation and they concluded

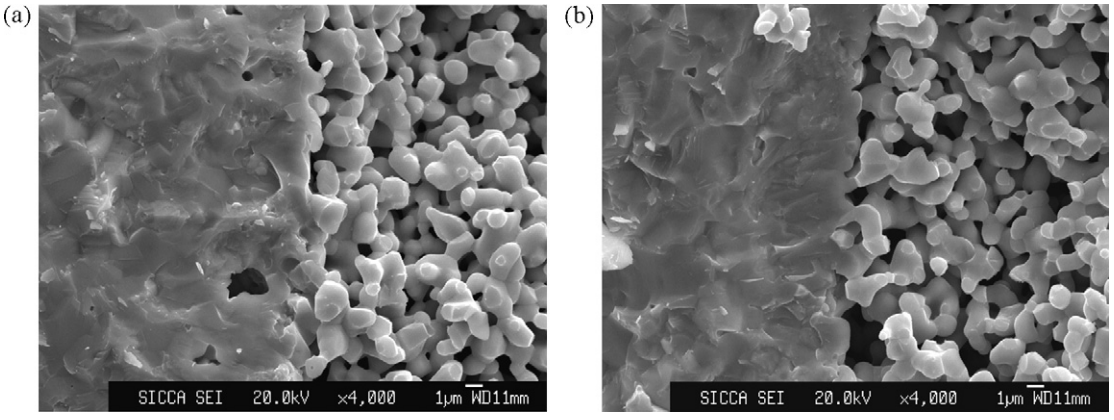

Fig. 10. FE-SEM micrograph of the interface LSGM/LSCM (a) and LSGMC/LSCM (b) after fuel cell test in ethanol steam at 750 °C for 60 h.

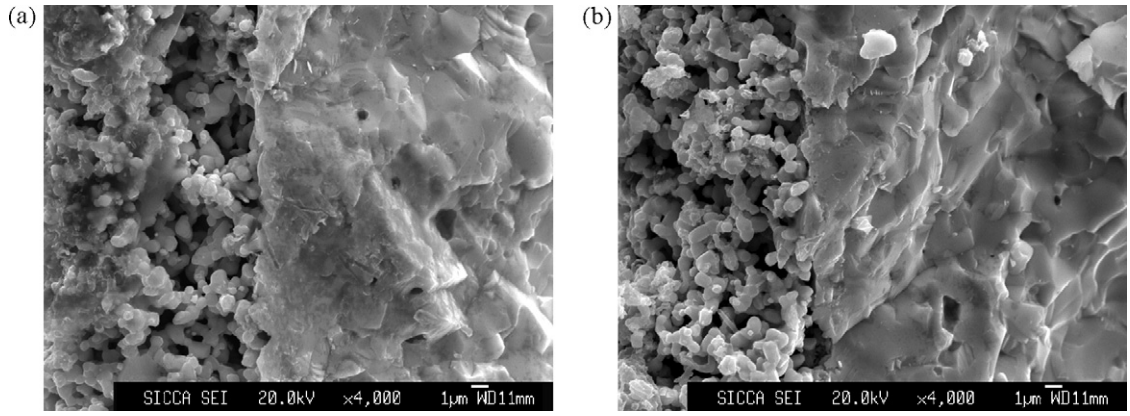

Fig. 11. FE-SEM micrograph of the interface LSGM/PCM (a) and LSGMC/PCM (b) after fuel cell test in ethanol steam at 750 °C for 60 h.

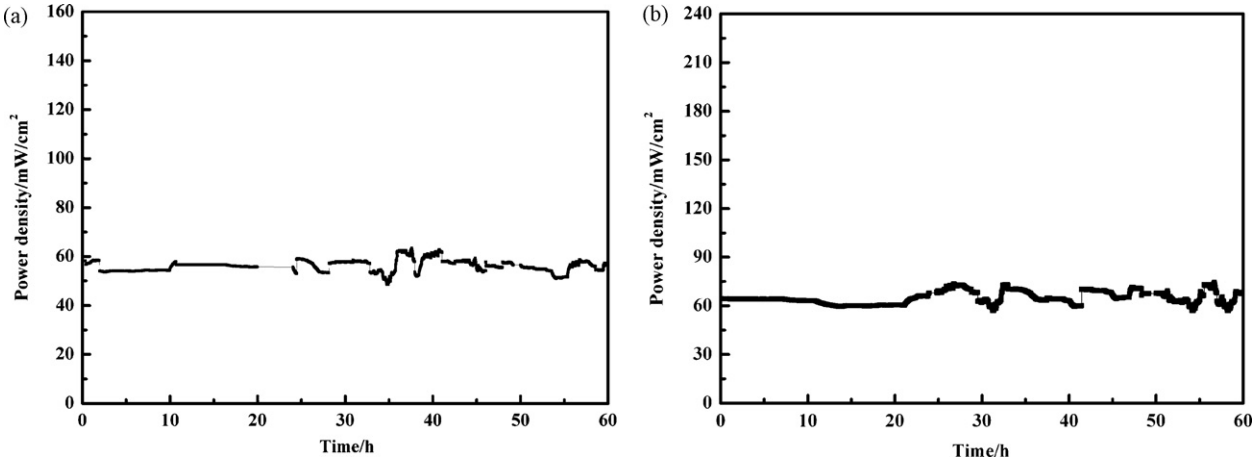

Fig. 12. Power density of a SOFC with the electrolyte-supported system LSCM/LSGM/PCM (a) and LSCM/LSGMC/PCM (b) using ethanol steam as fuel and oxygen as oxidant at 750 °C during the aging process.

that LSCM was a complete oxidation catalyst rather than a partial oxidation catalyst in methane oxidation as CO_2 dominates CO production [31]. Therefore, more work is required to do to study the steps and mechanism of ethanol oxidation by analyzing the components of the fuel effluent and improve performance of the cell running on ethanol fuel.

4. Conclusions

The electrochemical performance of LSCM/LSGM/PCM and LSCM/LSGMC/PCM cells were investigated in this study at different temperatures using humidified hydrogen or ethanol steam as fuels and oxygen as oxidant. The performance of LSCM/LSGMC/PCM was slightly superior to that obtained on LSCM/LSGM/PCM at different temperatures in both humidified hydrogen and ethanol steam atmospheres. The performance of the cell LSCM/LSGMC/PCM while operating on humidified hydrogen was modest with a maximum power density of 182 mW cm^{-2}, 125 mW cm^{-2} and 80 mW cm^{-2} at 850 °C, 800 °C and 750 °C, respectively, the corresponding values for the cell while operating on ethanol steam were 169 mW cm^{-2}, 120 mW cm^{-2} and 68 mW cm^{-2} with an electrolyte thickness of about 600 μm. Cell stability tests indicated no significant degradation in performance after 60 h of cell testing when LSCM anode was exposed to ethanol steam at 750 °C, suggesting that carbon deposition was limited during cell operation.

Acknowledgements

The authors thank the National "863" Program of China (No.2007AA05Z138) and the National Natural Science Foundation of China (No.50572062) for the grants that support this research.

References

[1] B.C.H. Steele, A. Heinzel, Nature 414 (2001) 345–352.
[2] T. Ishihara, J. Tabuchi, S. Ishikawa, J. Yan, M. Enoki, H. Matsumoto, Solid State Ionics 177 (2006) 1949–1953.
[3] R. Polini, A. Falsetti, E. Traversa, O. Sch¨af, P. Knauth, J. Eur. Ceram. Soc. 27 (2007) 4291–4296.
[4] R. Polini, A. Pamio, E. Traversa, J. Eur. Ceram. Soc. 24 (2004) 1365–1370.
[5] C. Lu, W.L. Worrell, C. Wang, S. Park, H. Kim, J.M. Vohs, R.J. Gorte, Solid State Ionics 152/153 (2002) 393.
[6] J. Liu, S.A. Barnett, Solid State Ionics 158 (2003) 11.
[7] J.-H. Koh, Y.-S. Yoo, J.-W. Park, H.C. Lim, Solid State Ionics 149 (2002) 157.
[8] J.B. Wang, J.-C. Jang, T.-J. Huang, J. Power Sources 122 (2003) 122.
[9] A. Atkinson, et al., Nat. Mater. 3 (2004) 17–27.
[10] S. Primdahl, J.R. Hansen, L. Grahl-Madsen, P.H. Larsen, J. Electrochem. Soc. 148 (2001) A74–A81.
[11] S.C. Singhal, K. Kendall, High Temperature Solid Oxide Fuel Cells: Fundamentals, Design and Applications, Elsevier, Oxford, 2004.
[12] Y. Matsuzaki, I. Yasuda, Solid State Ionics 132 (2000) 261–269.
[13] W.Z. Zhu, S.C. Deevi, Mater. Sci. Eng. A 362 (2003) 228–239.
[14] S. Park, J.M. Vohs, R.J. Gorte, Nature 404 (2000) 265–267.
[15] E. Perry, T. Tsai, S.A. Barnett, Nature 400 (1999) 649–651.
[16] C.H. Bartholomew, Catal. Rev. Sci. Eng. 24 (1982) 67.
[17] R.T.K. Baker, Carbon 27 (1989) 315.

[18] B.C.H. Steele, Solid State Ionics 86–88 (1996) 1223.
[19] K. Hernadi, A. Fonseca, J.B. Nagy, A. Siska, I. Kiricsi, Appl. Catal. A 199 (2000) 245.
[20] J.H. Koh, Y.-S. Yoo, J.-W. Park, H.C. Lim, Solid State Ionics 149 (2002) 157.
[21] T. Ishihara, T. Shibayama, S. Ishikawa, K. Hosoi, H. Nishiguchi, Y. Takita, J. Eur. Ceram. Soc. 24 (2004) 1329–1335.
[22] T. Ishihara, H. Furutani, M. Honda, T. Yamada, T. Shibayama, T. Akbay, N. Sakai, H. Yokokawa, Y. Takita, Chem. Mater. 11 (1999) 2081–2088.
[23] M. Mori, Y. Hier, J. Am. Ceram. Soc. 84 (2001) 2573.
[24] J. Vulliet, B. Morel, J. Laurencin, G. Gauthier, L. Bianchi, S. Giraud, J.Y. Henry, F. Lefebvre-Joud, S.C. Singhal, M. Dokiya (Eds.), SOFC-VIII, vol. 2003-07, The Electrochem. Soc, Pennington, NJ, 2003, p. 803.
[25] J. Sfeir, P.A. Buffat, P. Mockli, N. Xanthopoulos, R. Vasquez, H.J. Mathieu, J. Van herle, K.P. Thampi, J. Catal. 202 (2001) 229.
[26] J. Sfeir, J. Power Sources 118 (2003) 276.
[27] S. Tao, J.T.S. Irvine, Nat. Mater. 2 (2003) 320.
[28] S. Tao, J.T.S. Irvine, J. Electrochem. Soc. 151 (2004) A252.
[29] Bo Huang, S.R. Wang, R.Z. Liu, X.F. Ye, H.W. Nie, X.F. Sun, T.L. Wen, J. Power Sources 167 (2007) 39–46.
[30] Y. Du, N.M. Sammes, Proceedings of the 9th International Symposium on Solid Oxide Fuel Cells (SOFC-IX) PV 2005-07, The Electrochemical Society, 2005, p. 1127, ISBN: 1-56677-465-9.
[31] S.W. Tao, J.T.S. Irvine, S.M. Plint, J. Phys. Chem. B 110 (2006) 21771–21776.